






Optimization of 4-amino-pyridazin-3(2H)-one as a valid core scaffold for FABP4 inhibitors

Giuseppe Floresta¹  | Letizia Crocetti²  | Renan Rodrigues de Oliveira Silva³ |
Vincenzo Patamia¹  | Francesca Mazzacuva⁴ | Yu Chee Sonia Chen³ |
Claudia Vergelli²  | Agostino Cilibrizzi^{3,5} 

¹Department of Drug and Health Sciences, University of Catania, Catania, Italy

²Department of NEUROFARBA—Pharmaceutical and Nutraceutical Section, University of Florence, Florence, Italy

³Institute of Pharmaceutical Science, King's College London, London, UK

⁴School of Health, Sport and Bioscience, University of East London, London, UK

⁵Medicines Development, Centre for Therapeutic Innovation, University of Bath, Bath, UK

Correspondence

Letizia Crocetti, Department of Neurofarba,
Via Ugo Schiff 6, 50019 Sesto Fiorentino,
Firenze, Italy.

Email: letizia.crocetti@unifi.it

Agostino Cilibrizzi, Institute of Pharmaceutical
Science, King's College London, Stamford St,
London SE1 9NH, UK.

Email: agostino.cilibrizzi@kcl.ac.uk

Funding information

CAPES-PRINT, Grant/Award Number:
88887.570120/2020-00; Coordination for the
Improvement of Higher Education Personnel—
Brazil, Grant/Award Number: 88887.570120/
2020-00

Abstract

Current clinical research suggests that fatty acid-binding protein 4 inhibitors (FABP4is), which are of biological and therapeutic interest, may show potential in treating cancer and other illnesses. We sought to uncover new structures through the optimization of the previously reported 4-amino and 4-ureido pyridazinone-based series of FABP4is as part of a larger research effort to create more potent FABP4 inhibitors. This led to the identification of **14e** as the most potent analog with $IC_{50} = 1.57 \mu M$, which is lower than the IC_{50} of the positive control. Advanced modeling investigations and in silico absorption, distribution, metabolism, and excretion - toxicity calculations suggested that **14e** represents a potential candidate for in vivo studies such as FABP4i.

KEYWORDS

computing assisted molecular design, FABP4, FABP4 inhibitors, fatty acid binding protein, pyridazinone

1 | INTRODUCTION

Organic carboxylic acids with a long carbon chain known as fatty acids (FAs) have several roles in the body.^[1,2] Their persistently high quantity in the bloodstream causes a variety of diseases,^[3,4] including atherosclerosis, diabetes, and obesity. FAs are insoluble in water, due to the high lipophilicity of their chemical structure, and they must be transported into biological fluids by specific carriers so-called fatty acid-binding proteins (FABPs).^[5] Based on the location where they are found in the human body, FABPs have been classified into various families: A-FABP

(adipocyte), B-FABP (brain), E-FABP (epidermal), H-FABP (muscle and heart), I-FABP (intestinal), II-FABP (ileal), L-FABP (liver), M-FABP (myelin), and T-FABP (testis). FABP4 (aP2 or A-FABP) is the subtype predominantly expressed in adipocytes. When it was revealed that FABP4 knockout animal models showed protective effects against the development of insulin resistance as well as several pathological events linked to metabolic syndrome and atherosclerosis, research into small molecule inhibitors for this protein was first launched. Significantly, pharmacological therapies based on compounds that block the FABP4's normal activity are equally effective in this regard, showing comparable outcomes to genetic

This is an open access article under the terms of the Creative Commons Attribution License, which permits use, distribution and reproduction in any medium, provided the original work is properly cited.

© 2023 The Authors. *Archiv der Pharmazie* published by Wiley-VCH GmbH on behalf of Deutsche Pharmazeutische Gesellschaft.

methods by simulating the phenotype of FABP4-deficient animals.^[6] The development of cancer would also appear influenced by this family of transporter proteins,^[7] since several malignancies, including renal cell carcinoma, bladder cancer, prostate cancer, as well as other types of cancer cells, express FABPs nonphysiologically.^[8–10] Moreover, it was recently reported that FABP4 facilitates colon cancer metastasis and invasion and that administration of a conventional FABP4 small molecule inhibitor (BMS309403) reduced colon cancer cells' ability to migrate and invade.^[11] Additionally, FABP4 causes irregular metastatic patterns in ovarian cancer, and new studies show that the protein plays a role in the aggressiveness of this type of tumor, generating complications for its prognosis and treatment.^[12] Overall, this new body of evidence in the context of cancer research suggests that FABP4 targeting could offer new opportunities in the treatment of oncological conditions, in addition to the recognized effects on metabolic and cardiovascular conditions. Nevertheless, there are no FABP4 inhibitors (FABP4is) under clinical investigation at the present time.^[6,13] A potential and efficient tool for finding chemical hits such as FABP4i is computer-aided drug design.^[14–16] In line with our research focus in the discovery of novel bioactive heterocycles and the development of new anticancer agents,^[17,18] in this article, we describe the design, synthesis, and in vitro testing of novel heterocyclic small-molecule series as FABP4is, derived from the structural optimization of our recently reported 4-amino and 4-ureido pyridazinone-based inhibitors.^[19]

2 | RESULTS AND DISCUSSION

2.1 | Chemistry

2.1.1 | Heterocyclic small-molecule design

As shown in Figure 1, recently we took use of a two-step computationally assisted molecular design to find novel FABP4i scaffolds starting from the bioisosteric-replacement/scaffold-hopping of the pyrimidine core of the cocrystallized ligand (i.e., 2-[(2-oxo-2-piperidin-1-ylethyl)sulfanyl]-6-(trifluoromethyl)pyrimidin-4-ol; PBDID: 1TOU). Our examination of bioisosteric replacement resulted in the choice of 4-amino and 4-ureido pyridazinone as a suitable scaffold to

develop a series of FABP4is with low micromolar activities.^[19] In this work we have further optimized the structure of the identified scaffold, leading to new inhibitors with increased potency. We have carried out a scaffold hopping analysis as reported in Figure 1 and then scored the compounds with Molecular Mechanics Poisson-Boltzmann Surface Area (MM/PBSA) calculations, as described in the section (see Supporting Information Material for details of the selection criteria for the in vitro evaluation of the compounds). This approach has enabled the selection of 25 target molecules. The compounds were then synthesized and the 13 predicted as most active (see Supporting Information: Table S1) were screened against FABP4 in vitro. The chemical structures of the new series of compounds are reported in Tables 1 and 2.

2.1.2 | Chemistry

All intermediates and final compounds were synthesized as reported in Schemes 1–3 and the structure were confirmed on the basis of analytical and spectral data.

Scheme 1 shows the synthetic pathways affording the final products of type 3, 6, and 7, in which position 2, 4, 5, and 6 of pyridazinone were suitably modified to introduce selected residues of interest. For the synthesis of compounds 3a–h, intermediates 1a–c^[20–22] were reacted with cerium ammonium nitrate (CAN) in a mixture of 50% AcOH and 65% HNO₃, adopting a previously established procedure,^[23] affording intermediates 2a,b^[22,24] and the new 2c. The displacement of the nitro group with suitable alkyl- or heteroarylamine lead to the desired final compounds of type 3. For the synthesis of final compounds 7a,b, the intermediate 1c^[22] was converted into compound 4 adopting previously established reduction conditions with ammonium formate and 10% Pd/C in EtOH.^[25] Subsequently, the treatment of 4 with bromine and 47% HBr in glacial acetic acid afforded intermediate 5, which was reacted with thioacetamide in ethanol to give the final compound 6. Compounds 7a,b were then obtained from 6 through coupling reaction with the appropriate aryl boronic acid in the presence of dry cupric acetate and triethylamine in anhydrous CH₂Cl₂.

In Scheme 2 is reported the synthesis of the final compounds 11a,b featuring a pyridazine scaffold in the place of the pyridazinone.

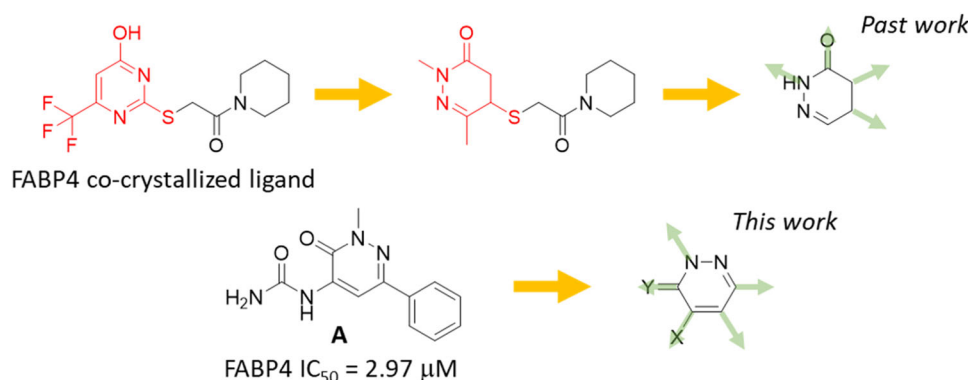
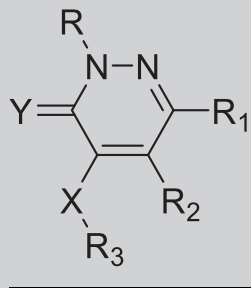


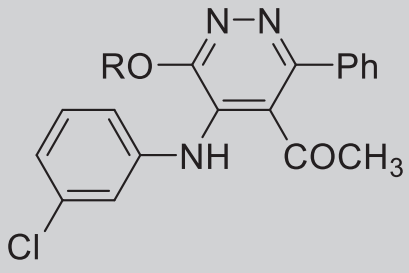
FIGURE 1 Computer-aided design of the new scaffolds shown schematically. Y = O, S, X = NH, CH₂.

TABLE 1 Structures of final compounds of type **3**, **6**, **7**, **14**, **15**, and **17**.


Comp.	R	R ₁	R ₂	R ₃	X	Y
3a	CH ₂ Ph	Ph	COCH ₃	C ₂ H ₅	NH	O
3b	CH ₂ Ph	Ph	COCH ₃	iC ₃ H ₇	NH	O
3c	CH ₂ Ph	Ph	COCH ₃	CH ₃	NH	O
3d	C ₂ H ₅	Ph	COCH ₃	adamantan-1-yl	NH	O
3e	C ₂ H ₅	Ph	COCH ₃	CH ₂ -3-Py	NH	O
3f	C ₂ H ₅	Ph	COCH ₃	CH ₂ -2-Py	NH	O
3g	C ₂ H ₅	Ph	COCH ₃	(CH ₂) ₂ -2-Py	NH	O
3h	C ₂ H ₅	CH ₃	COCH ₃	3-Py	NH	O
6	C ₂ H ₅	CH ₃	thiazol-4-yl	H	NH	O
7a	C ₂ H ₅	CH ₃	thiazol-4-yl	4-CN-Ph	NH	O
7b	C ₂ H ₅	CH ₃	thiazol-4-yl	3,4,5-F-Ph	NH	O
14a	C ₂ H ₅	Ph	H	Ph	CH ₂	O
14b	C ₂ H ₅	Ph	H	3-F-Ph	CH ₂	O
14c	C ₂ H ₅	Ph	H	3-Cl-Ph	CH ₂	O
14d	C ₂ H ₅	Ph	H	3-Br-Ph	CH ₂	O
14e	C ₂ H ₅	Ph	H	3-OCH ₃ -Ph	CH ₂	O
14f	C ₂ H ₅	Ph	H	2-OCH ₃ -Ph	CH ₂	O
14g	C ₂ H ₅	Ph	H	naphtalen-2-yl	CH ₂	O
14h	C ₂ H ₅	4-F-Ph	H	3-Cl-Ph	CH ₂	O
15	C ₂ H ₅	Ph	H	3-Cl-Ph	CH ₂	S
16a	C ₂ H ₅	Ph	H	4-COOEt-Ph	CH ₂	O
16b	C ₂ H ₅	Ph	H	2-COOEt-Ph	CH ₂	O
17	C ₂ H ₅	Ph	H	4-COOH-Ph	CH ₂	O

Intermediate **8**^[26] was treated with the suitable alcoholate to give the isoxazolopyridazines **9a,b** (for **9b**^[26]). The reductive cleavage with 10% Pd/C in Parr instrument at 60 Psi gave 4-amino-5-acetyl derivatives **10a,b**, which were in turn coupled with 3-chlorophenylboronic acid following the same conditions previously described for **7a,b**.

Scheme 3 depicts the synthetic procedures adopted to obtain the final products **14a–h**, **15**, **16a,b**, and **17**, showing various functional groups in position 4 of the pyridazinone. Through condensation with the appropriate aromatic aldehyde in the presence of KOH, dihydropyridazinones **12a,b**^[27] were firstly converted into

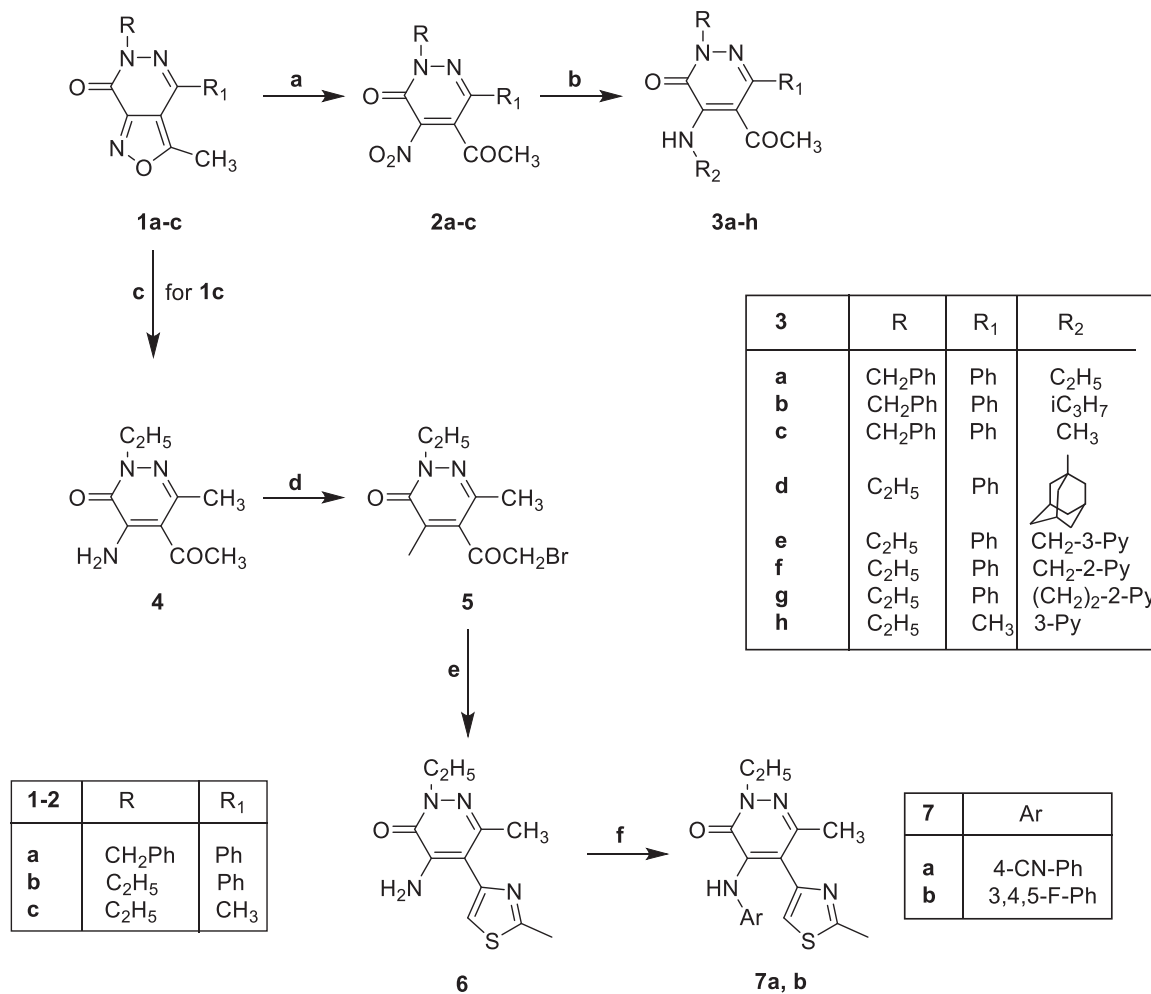
TABLE 2 Structures of the final compounds **11a,b**.


Comp.	R
11a	CH ₃
11b	C ₂ H ₅

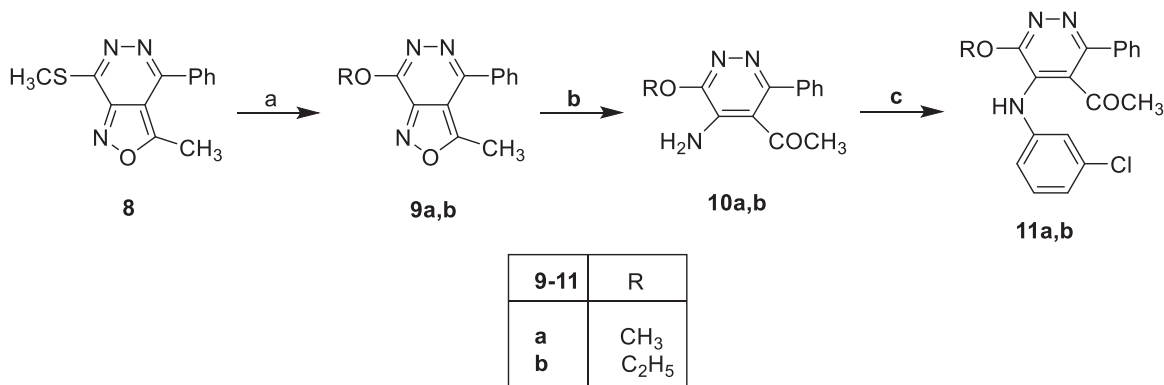
the previously described 4-benzyl derivatives **13a–g**^[28–32] and in the new analogs **13h–j**. Subsequently, compounds of type **13** were finally alkylated with ethyl bromide in anhydrous dimethylformamide (DMF) under standard conditions to give final compounds **14a–h** and **16a,b**. For **16a,b**, these reaction conditions produced also the esterification of the carboxylic group in the *para* (**13i**) or *ortho* (**13j**) position of the benzyl group, simultaneously to the alkylation of N-1 on the pyridazinone. Lastly, compound **15** was obtained from intermediate **14c** through treatment with Lawesson's reagent in anhydrous toluene, while the hydrolysis of **16a** with 6 N NaOH in EtOH afforded the final compound **17**.

2.2 | FABP4 inhibition evaluation

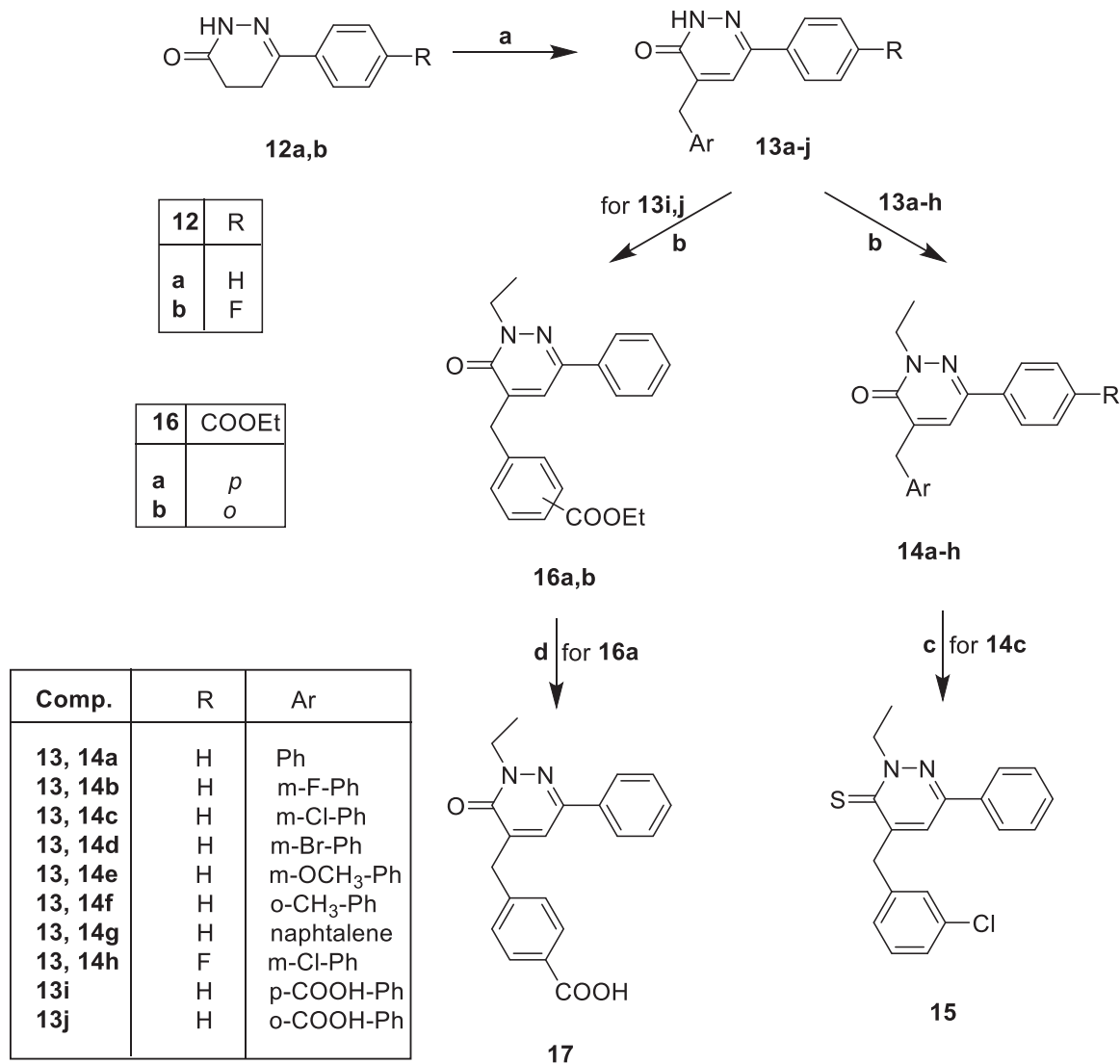
The reduction in fluorescence signal of when a powerful FABP4 ligand displaces a detection reagent (DR), was used to measure the FABP4 inhibitory activity. When bound to FABP4, the DR displays a higher fluorescence intensity. Therefore, a decrease in the fluorescence read-out is caused by any ligand that can successfully bind to the same binding pocket and has the ability to displace the DR. The new molecular series was examined in two steps. First, an assessment of the inhibitory effect of all the compounds was obtained using a single dose of 5 μM. Then, only the substances that could lower the fluorescence reading by at least 95% were assessed further, by measuring the IC₅₀ values (μM), which were then contrasted with the arachidonic acid's activity (i.e., FABP4 established ligand). Figure 2 reports the single-point displacement results. Based on the data of the first screening, four molecules were selected as the analogs with higher efficacy—that is, able to reduce the fluorescence of the DR to at least 95%, worth to be progressed to IC₅₀ calculation. In IC₅₀ experiments, using arachidonic acid as a positive control, IC₅₀ of 3.30 μM was obtained. Table 3 lists the IC₅₀ values for the compounds in our set. Molecule **14e** revealed a strong inhibitory effect, with an IC₅₀ value (i.e., 1.57 μM) value lower than the standard arachidonic acid and lower than the previous FABP4i that we had found (compound **A**,^[19] Figure 1).



SCHEME 1 Synthesis of compounds **3a-h**, **6**, and **7a,b**. Reagents and conditions: (a) CAN, 50% AcOH, 65% HNO₃, 55°C, 30 min. (b) Alkyl or heteroarylamine, EtOH, r.t., 30 min–2 h. (c) HCOONH₄, 10% Pd/C, EtOH, reflux, 1 h. (d) 47% HBr, glacial AcOH, Br₂, 50°C, 90 min. (e) Thioacetamide, EtOH, reflux, 1 h. (f) Aryl boronic acid, anhydrous cupric acetate, triethylamine, activated molecular sieves, anhydrous CH₂Cl₂, r.t., 5–24 h.



SCHEME 2 Synthesis of compounds **11a,b**. Reagents and conditions: (a) RONA, abs. EtOH, r.t., 3 h. (b) 10% Pd/C, EtOH, Parr instrument at 60 PSI, r.t., 5 h. (c) 3-Chlorophenylboronic acid, anhydrous cupric acetate, triethylamine, activated molecular sieves, anhydrous CH₂Cl₂, r.t., 3–4 h.



SCHEME 3 Synthesis of compounds **14a-h**, **15**, **16a,b**, and **17**. Reagents and conditions: (a) 5% (w/v) KOH, abs. EtOH, 2- or 4-carboxybenzaldehyde, r.t., 1-2 h. (b) Ethyl bromide, K₂CO₃, anhydrous DMF, 80°C, 1 h. (c) Lawesson's reagent, anhydrous toluene, reflux, 7 h. (d) 6 N NaOH, EtOH, r.t., 1 h.

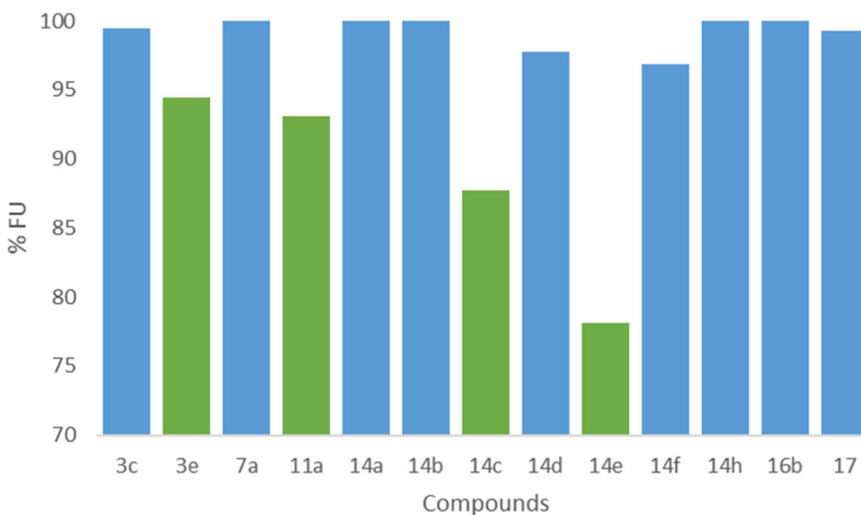


FIGURE 2 Single point displacement experiment for selected compounds.

2.3 | Molecular docking and ADMET prediction

Since the first apo-FABP crystal structure was published in 1992, numerous different holo-FABP structures with a variety of ligands have been discovered. It is now established, that the side chains of the FABP hydrophobic pocket form a hydrogen bond with the carboxylate of the FAs toward various amino acidic residues. Furthermore, these interactions may be mediated by a network of water molecules. Figure 3 shows the interactions for the most active compounds identified in this study—that is, **3e**, **11a**, **14c**, and **14e** (two-dimensional [2D] interactions are reported in the Supporting Information: Figures S1–S4). Each compound has many interactions with the appropriate residues in the binding pocket, for instance, Y128 and R106. As shown in the Figure 3, compounds **3e**, **14c**, and **14e** prefer a binding pose where the carbonyl of the central core interacts with R126 and the other aromatic rings are allocated in the additional hydrophobic pockets, in a binding pose similar to that of

the starting reference compound (Figure 1). In contrast, analog **11a** does not interact with R126, rather a hydrogen bond is formed between this analog and S53 (See Supporting Information: Figure S2). This missing interaction with R126 may explain the compound's decreased activity, as seen by the lower binding energy interaction.

The stability over time of the most potent molecule was further investigated by molecular dynamic (MD) experiments. One hundred nanoseconds of simulation were run in explicit water at neutral pH (7.4) as described in the experimental part. The results of the simulation confirmed that molecule **14e** is able to maintain the binding poses over time, as determined by the calculated root mean square deviation (RMSD) that maintain a constant level (Figure 4), after the initial stabilization of the starting structure (0 ns). As expected, the protein structure is also not influenced by the binding of molecule **14e**, confirming a certain degree of stability of the protein-**14e** complex (see Supporting Information: Figure S5). Using FABP3 crystallized protein,^[33] the possible activity of our compounds against FABP3 was investigated through docking studies. To validate the calculation of the binding affinity we used five compounds as reference for which the experimental K_i toward FABP3 was reported.^[34] The results have been reported in Supporting Information: Table S4, from which it is possible to deduce that our compounds **3e**, **11a**, **14c**, and **14e** have very low activity against FABP3.

By examining pharmacokinetic profiles and potential negative side effects of **14e**, the in silico assessment has been enhanced. The ability to reach targets in bioactive form was assessed using the SwissADME (<http://swissadme.ch>) and pkCSM (<http://biosig.unimelb.edu.au/pkcsm/>) web platforms. SwissADME results are reported in Supporting Information: Table S2 and pkCSM results are reported in Supporting Information:

TABLE 3 Measured IC_{50} values for selected compounds.

Compounds	IC_{50} (μ M)
3e	6.20 ± 0.42
11a	13.68 ± 0.54
14c	5.55 ± 0.22
14e	1.57 ± 0.26
Arachidonic acid	3.30 ± 0.27

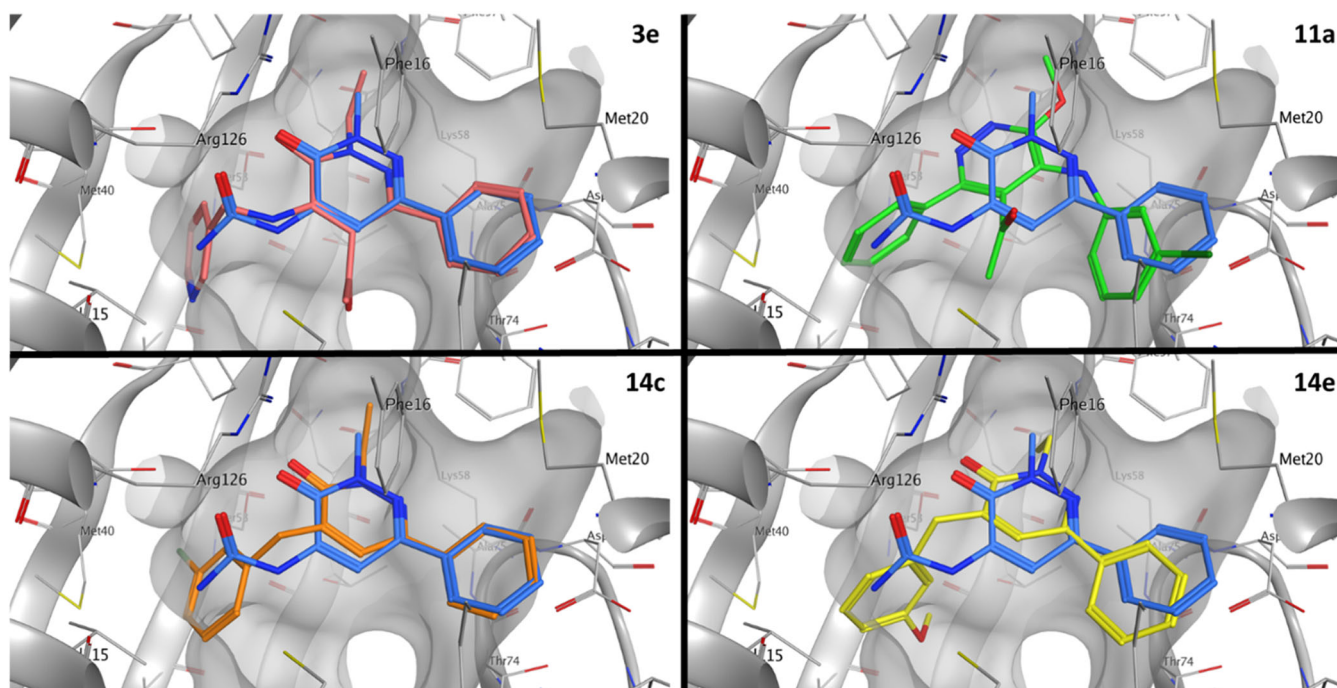


FIGURE 3 **3e** (red), **11a** (green), **14c** (orange), and **14e** (yellow) poses inside the binding pocket of fatty acid-binding protein 4 (FABP4) compared with the reference compound (blue; see Figure 1 for molecular structure).

Solute RMSD from the starting structure

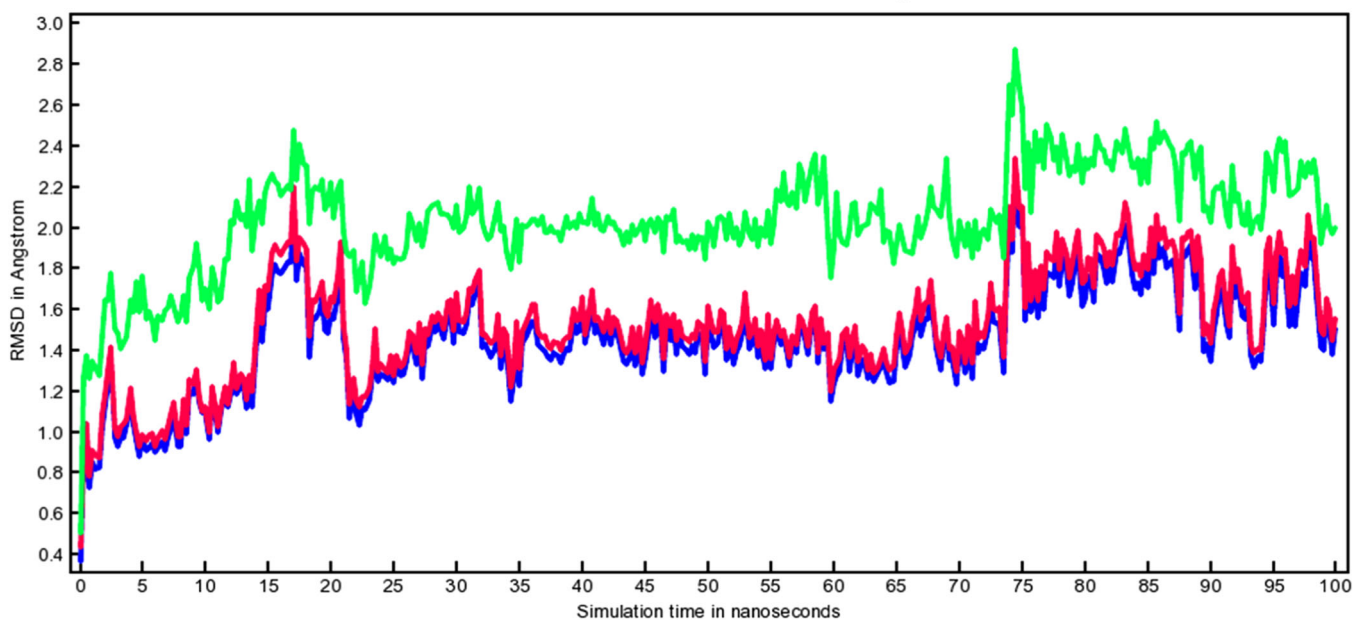


FIGURE 4 Solute RMSD from the starting structure as a function of simulation time. Fatty acid-binding protein 4 (FABP4) in blue. **14e** in red. All the simulated system in green.

Table S3. From these experiments, the compound results orally available and moderately soluble in water. **14e** resulted as a Pgp substrate and no violation to the Lipinski rule of 5 is reported. Other four drug-likeness rules named Ghose, Egan, Veber, and Muegee, were simultaneously satisfied. The result of the PAINS interference structures model assay, that was designed to exclude molecules that are most likely to show false positives in biological assays, did not point out any inconsistency. The calculated absorption and distribution have been graphically represented by the Edan-Egg model reported in Supporting Information: Figure S10 (Brain or Intestinal Estimated, BOILED-Egg). The visual analysis of the Edan-Egg model highlights that **14e** was predicted to passively permeate the blood-brain barrier. Regarding the absorption parameters, the compound presents a promising oral availability due to the optimal Caco-2 cell permeability and intestinal absorption. Additionally, the molecule is anticipated to be available to interact with the pharmaceutical target because of the plasma's high unbound proportion. The calculated value of total clearance indicates that **14e** has a good renal elimination and is a substrate of the renal organic cation transporter 2. Lastly, the compound did not pass the AMED toxicity test (and it could be hepatotoxic), whereas no skin sensitization is recorded. The max tolerated human dose is 0.328 (log mg/kg/day).

3 | CONCLUSION

We have optimized a previous series of FABP4 inhibitors based on 4-amino- and 4-ureido-pyridazinone scaffolds,^[19] the design of which was directed by bioisosteric-replacements/scaffold hopping and evaluated by MM/GBSA calculations. Twenty-five new best-scoring

molecules have been synthesized and the most active hits were further biologically evaluated for their FABP4 inhibitory activity. The structural optimization of our previous series led to the identification of several new analogs (e.g., **3e**, **11a**, **14c**, **14e**) with higher FABP4 inhibitory activity (i.e., IC_{50} in the low micromolar range) than the former compounds. In particular, **14e** resulted in the most potent analog, with $IC_{50} = 1.57 \mu\text{M}$, which is lower than the IC_{50} of the positive control (arachidonic acid, $IC_{50} = 3.30 \mu\text{M}$). MD experiments confirmed the capability of **14e** to establish interactions with several amino acids into FABP4 binding pocket, being this in agreement with the higher activity recorded in vitro for **14e**, in comparison to the other analogs developed in this study. Lastly, in silico absorption, distribution, metabolism, and excretion - toxicity (ADMET) calculations suggested that **14e** would be optimally absorbed, distributed, metabolized, and excreted, as well as well adsorbed by the skin and intestine, having the potential to enable topical and oral route of administration during future in vivo studies as FABP4i.

4 | EXPERIMENTAL

4.1 | Chemistry

4.1.1 | General

All the chemical reagents were purchased from Merck and Sigma Aldrich of reagent grade and were used without any further purification. Extracts were dried over Na_2SO_4 and the solvents were removed under reduced pressure. All reactions were monitored by thin layer chromatography

(TLC) using commercial plates (Merck) precoated with silica gel 60 F-254. Visualization was performed by UV fluorescence ($\lambda_{\text{max}} = 254 \text{ nm}$) or by staining with iodine or potassium permanganate. Chromatographic separations were performed on silica gel columns by gravity (Kieselgel 40, 0.063–0.200 mm; Merck) or flash chromatography (Kieselgel 40, 0.040–0.063 mm; Merck). Yields refer to chromatographically and spectroscopically pure compounds, unless otherwise stated. When reactions were performed in anhydrous conditions, the mixtures were maintained under nitrogen atmosphere. Compounds were named following International Union of Pure and Applied Chemistry rules as applied by Beilstein-Institut AutoNom 2000 (4.01.305) or CA Index Name. All melting points were determined on a microscope hot stage Büchi apparatus and are uncorrected. $^1\text{H-NMR}$ and $^{13}\text{C-NMR}$ spectra were obtained on a Bruker AVANCE 400 spectrometer at 400 and 100 MHz respectively using 5 mm internal diameter glass tubes. Chemical shifts (δ) values are expressed as parts per million (ppm) using DMSO (d_6) (2.50 for proton and 39.52 for carbon), methanol (d_4) (3.31 for proton and 49.00 for carbon) or CDCl_3 (7.26 for proton and 77.16 for carbon) as solvents. The coupling constants (J) are reported in Hertz. The following splitting patterns are identified: s, singlet; d, doublet; t, triplet; m, multiplet, or any combination of these, for example, dd, dt, and so on. Analytical reversed-phase high-performance liquid chromatography (reversed-phase HPLC) was conducted out on HP 1050 instrument (Agilent Technologies) to ascertain the chromatographic purity of compounds. The system includes a quaternary pump, an autosampler, and a Kontron DEG 104 degasser (Kontron). A C_{18} column, Zorbax, 80 Å, 3.5 μm , 2.1 \times 100 mm was used with a total run time of 30 min. The mobile phase is composed of 0.1% trifluoroacetic acid (TFA) in Milli-Q H_2O and acetonitrile (ACN) at a flow rate of 0.3 mL/min with an injection volume was 10–30 μm . The compounds were detected at 281 and 254 nm UV wavelengths. The values of the retention times (t_{R}) are given in minutes. All final compounds progressed to biological tests resulted in a purity of $\geq 95\%$. Mass spectrometry (LC-MS) experiments were performed on all the samples. The stock solutions (1 mg/mL in MeOH) were diluted with 0.1% HCOOH in MeOH/ H_2O (50:50) to a final concentration of 50 $\mu\text{g/mL}$ before analysis. The instrument used consisted of a Thermo Accela LC system interfaced to a Thermo TSQ Access triple quadrupole mass spectrometer with a heated electrospray ionization source. The data were processed with Xcalibur software (version 2.0). A total of 10 μL of the sample were analyzed in flow injection, with a flow rate of 0.2 mL/min of mobile phase 0.1% HCOOH in MeOH/ H_2O (50:50). Parameters used for the analysis in positive ion mode were: spray voltage 3500 V; vaporizer temperature 300°C; sheath gas pressure 50 au; capillary temperature 350°C; capillary offset 35. Microanalyses were performed with a Perkin-Elmer 260 elemental analyzer for C, H, and N, and they were within $\pm 0.4\%$ of the theoretical values.

4.1.2 | Synthesis of 5-acetyl-2-ethyl-6-methyl-4-nitropyridazin-3(2H)-one **2c**

CAN (6.20 mmol) was portion-wise added to a stirred suspension of isoxazolo[3,4-*d*]pyridazinone **1c**^[22] (0.78 mmol) in a mixture of 50%

AcOH (5 mL) and 65% HNO_3 (1 mL) at 55°C over a period of 30 min. The addition of ice water (20 mL) produced a suspension which was extracted with CH_2Cl_2 (3 \times 10 mL). After evaporation of the solvent the residue was purified by column chromatography using cyclohexane/ethyl acetate 1:2 as eluent. Yield = 57%; mp = 103–107°C (EtOH). $^1\text{H-NMR}$ (400 MHz, CDCl_3) δ 4.31 (q, $J = 7.2 \text{ Hz}$, 2H, CH_2), 2.59 (s, 3H, CH_3CO), 2.34 (s, 3H, C6- CH_3), 1.43 (t, $J = 7.2 \text{ Hz}$, 3H, CH_3). Anal. Calcd $\text{C}_9\text{H}_{11}\text{N}_3\text{O}_4$ (225.20): C, 48.00; H, 4.92; N, 18.66; found: C, 48.11; H, 4.91; N, 18.61.

4.1.3 | General procedure for the synthesis of compounds **3a–h**

To a stirred solution of suitable 5-acetyl-4-nitropyridazin-3(2H)-one of type **2** (**2a**^[24]; **2b**^[22]) (0.34 mmol) in 2–3 mL of ethanol, the appropriate alkyl- or heteroaryl- amine (0.34–0.68 mmol) was added portion-wise. The resulting mixture was stirred at room temperature for 30 min to 2 h. For compound **3d**, the mixture was refluxed for 3 h. After cooling, the final product was collected by filtration and recrystallized from ethanol. For compounds **3a**, **3b**, and **3g**, after the concentration of the solvent, water was added (10 mL) and the mixture was extracted with CH_2Cl_2 (3 \times 15 mL). The organic phase was dried over Na_2SO_4 and evaporated to give the final compounds, which were purified by flash chromatography using cyclohexane/ethyl acetate 3:1 (for **3a,b**) and cyclohexane/ethyl acetate 1:2 (for **3g**) as eluents.

5-Acetyl-2-benzyl-4-(ethylamino)-6-phenylpyridazin-3(2H)-one (3a)
Yield = 40%; mp = 93–95°C (EtOH). $^1\text{H-NMR}$ (400 MHz, CDCl_3) δ 7.60–7.22 (m, 10H, Ar), 7.12 (exch br s, 1H, NH), 5.35 (s, 2H, $\text{CH}_2\text{-Ph}$), 3.32 (q, $J = 7.2 \text{ Hz}$, 2H, CH_2), 1.88 (s, 3H, COCH_3), 1.23 (t, $J = 7.2 \text{ Hz}$, 3H, CH_3). Anal. Calcd $\text{C}_{21}\text{H}_{21}\text{N}_3\text{O}_2$ (347.42): C, 72.60; H, 6.09; N, 12.10; found: C, 72.38; H, 6.08; N, 12.13.

5-Acetyl-2-benzyl-4-(isopropylamino)-6-phenylpyridazin-3(2H)-one (3b)
Yield = 30%; mp = 126–128°C (EtOH). $^1\text{H-NMR}$ (400 MHz, CDCl_3) δ 7.85 (exch br s, 1H, NH), 7.60–7.23 (m, 10H, Ar), 5.36 (s, 2H, $\text{CH}_2\text{-Ph}$), 4.42 (m, 1H, CH), 1.86 (s, 3H, COCH_3), 1.21 (s, 3H, CH_3), 1.19 (s, 3H, CH_3). Anal. Calcd $\text{C}_{22}\text{H}_{25}\text{N}_3\text{O}_2$ (361.45): C, 73.11; H, 6.41; N, 11.63; found: C, 73.29; H, 6.40; N, 11.66.

5-Acetyl-2-benzyl-4-(methylamino)-6-phenylpyridazin-3(2H)-one (3c)
Yellow-colored solid, mp = 153–155°C (EtOH). Yield = 34%. $^1\text{H-NMR}$ (400 MHz, CDCl_3) δ 7.49 (s, 1H, NH), 7.47 (s, 1H, Ar), 7.43–7.39 (m, 5H, Ar), 7.36–7.29 (m, 4H, Ar), 5.33 (s, 2H, CH_2), 2.94 (s, 3H, CH_3), 1.88 (s, 3H, CH_3). $^{13}\text{C-NMR}$ (100 MHz, CDCl_3) δ 202.21, 137.31, 136.36, 129.28, 128.90, 128.77, 128.67, 128.00, 56.02, 33.32, 32.50. MS-ESI for $\text{C}_{20}\text{H}_{19}\text{N}_3\text{O}_2$ (calcd. 333.15), $[\text{M}+\text{H}]^+$ at m/z 333.92. Anal. Calcd $\text{C}_{20}\text{H}_{19}\text{N}_3\text{O}_2$ (333.39): C, 72.05; H, 5.74; N, 12.60; found: C, 72.24; H, 5.73; N, 12.57.

5-Acetyl-4-[[[(3,5,7-s)-adamantan-1-yl]amino]-2-ethyl-6-phenylpyridazin-3(2H)-one (3d)

Yield = 56%; mp = 124–125°C (EtOH). ¹H-NMR (400 MHz, CDCl₃) δ 9.08 (exch br s, 1H, NH), 7.45 (s, 5H, Ar), 4.25 (q, J = 7.6 Hz, 2H, CH₂), 2.21–2.02 (m, 9H, adamant), 1.80 (s, 3H, COCH₃), 1.71–1.60 (m, 6H, adamant), 1.41 (t, J = 7.6 Hz, 3H, CH₃). Anal. Calcd C₂₄H₂₉N₃O₂ (391.52): C, 73.63; H, 7.47; N, 10.73; found: C, 73.81; H, 7.46; N, 10.70.

5-Acetyl-2-ethyl-6-phenyl-4-[(pyridin-3-ylmethyl)amino]pyridazin-3(2H)-one (3e)

Yellow-colored solid, mp = 162–163°C (EtOH). Yield = 58%. ¹H-NMR (400 MHz, CDCl₃) δ 8.54 (s, 2H, Ar), 8.02 (exch br s, 1H, NH), 7.70 (d, J = 8.0 Hz, 1H, Ar), 7.41–7.33 (m, 6H, Ar), 4.77 (d, J = 6.4 Hz, 2H, CH₂), 4.23 (q, J = 7.2 Hz, 2H, CH₂), 1.58 (s, 3H, COCH₃), 1.41 (t, J = 7.2 Hz, 3H, CH₃). ¹³C-NMR (100 MHz, CDCl₃) δ 202.07, 155.89, 148.30, 148.16, 146.36, 140.79, 137.54, 136.45, 134.46, 129.39, 129.00, 128.64, 124.16, 113.71, 47.70, 46.33, 32.27, 13.45. MS-ESI for C₂₀H₂₀N₄O₂ (calcd. 348.16), [M+H]⁺ at m/z 349.04, t_R = 10.453. Anal. Calcd C₂₀H₂₀N₄O₂ (348.16): C, 68.95; H, 5.79; N, 16.08; found: C, 68.77; H, 5.78; N, 16.04.

5-Acetyl-2-ethyl-6-phenyl-4-[(pyridin-2-ylmethyl)amin]pyridazin-3(2H)-one (3f)

Yield = 42%; mp = 138–140°C (EtOH). ¹H-NMR (400 MHz, CDCl₃) δ 8.77 (exch br m, 1H, NH), 8.65 (m, 2H, Ar), 7.44–7.29 (m, 1H, Ar), 7.41 (s, 5H, Ar), 7.27 (m, 2H, Ar), 4.71 (d, 2H, J = 4.8 Hz, CH₂), 4.28 (q, J = 7.4 Hz, 2H, CH₂), 1.81 (s, 3H, COCH₃), 1.43 (t, J = 7.4 Hz, 3H, CH₃). Anal. Calcd C₂₀H₂₀N₄O₂ (348.16): C, 68.95; H, 5.79; N, 16.08; found: C, 68.79; H, 5.80; N, 16.03.

5-Acetyl-2-ethyl-6-phenyl-4-[[2-(pyridin-2-yl)ethyl]amino]pyridazin-3(2H)-one (3g)

Yield = 90%; oil. ¹H-NMR (400 MHz, CDCl₃) δ 8.57 (m, 2H, Ar), 7.78 (exch br m, 1H, NH), 7.65 (m, 1H, Ar), 7.39 (s, 5H, Ar), 7.26–7.14 (m, 2H, Ar), 4.71 (d, J = 4.8 Hz, 2H, N-CH₂), 4.25–4.14 (q, J = 7.2 Hz, 2H, CH₂), 3.77–3.68 (m, 2H, N-CH₂), 3.16–3.09 (t, J = 6.6 Hz, 2H, CH₂), 1.86 (s, 3H, COCH₃), 1.37 (t, J = 7.2 Hz, 3H, CH₃). Anal. Calcd C₂₁H₂₂N₄O₂ (362.17): C, 69.59; H, 6.12; N, 15.46; found: C, 69.78; H, 6.11; N, 15.42.

5-Acetyl-2-ethyl-6-methyl-4-(pyridin-3-ylamino)pyridazin-3(2H)-one (3h)

Yield = 43%; mp = 156–158°C (EtOH). ¹H-NMR (400 MHz, CDCl₃) δ 8.64 (exch br s, 1H, NH), 8.37 (m, 2H, Ar), 7.45 (m, 2H, Ar), 4.24–4.15 (q, J = 7.2 Hz, 2H, CH₂), 2.23 (s, 3H, C6-CH₃), 2.14 (s, 3H, CH₃CO), 1.44–1.37 (t, J = 7.2 Hz, 3H, CH₃). Anal. Calcd C₁₄H₁₆N₄O₂ (372.31): C, 61.75; H, 5.92; N, 20.58; found: C, 61.92; H, 5.94; N, 20.52.

4.1.4 | Synthesis of 5-acetyl-4-amino-2-ethyl-6-methylpyridazin-3(2H)-one 4

A mixture of 6-ethyl-3,4-dimethylisoxazolo[3,4-d]pyridazin-7(6H)-one **1c** (1.29 mmol),^[22] 10% Pd/C (62 mg) and ammonium formate (4 mmol) in ethanol (5 mL) was refluxed for 1 h. After the addition of CH₂Cl₂

(10 mL) the catalyst was filtered off and the solvent was removed under reduced pressure to yield compound **4**, which was purified by crystallization from ethanol. Yield = 98%; mp = 102–104°C (EtOH). ¹H-NMR (400 MHz, CDCl₃) δ 7.74 (exch br s, 2H, NH₂), 4.16–4.05 (q, J = 7.2 Hz, 2H, CH₂), 2.54 (s, 3H, C6-CH₃), 2.48 (s, 3H, CH₃CO), 1.33 (t, J = 7.2 Hz, 3H, CH₃). Anal. Calcd C₉H₁₃N₃O₂ (195.22): C, 55.37; H, 6.71; N, 21.52; found: C, 55.23; H, 6.72; N, 21.59.

4.1.5 | Synthesis of 4-amino-5-(2-bromoacetyl)-2-ethyl-6-methylpyridazin-3(2H)-one 5

To a stirred solution of compound **4** (0.80 mmol) and a catalytic amount of 47% HBr in glacial acetic acid (2.5 mL), a solution of Br₂ (0.80 mmol) in glacial acetic acid (1.5 mL) was portion-wise added over 30 min. The mixture was heated to 50°C for 90 min. After cooling ice-cold water was added and the precipitate was recovered by filtration. Yield = 92%; mp = 120–121°C (EtOH). ¹H-NMR (400 MHz, CDCl₃) δ 7.82 (exch br s, 2H, NH₂), 4.40 (s, 2H, CH₂Br), 4.16 (q, J = 7.2 Hz, 2H, CH₂), 2.61 (s, 3H, C6-CH₃), 1.40 (t, J = 7.2 Hz, 3H, CH₃). Anal. Calcd C₉H₁₂BrN₃O₂ (274.12): C, 39.44; H, 4.41; N, 15.33; found: C, 39.56; H, 4.40; N, 15.30.

4.1.6 | Synthesis of 4-amino-2-ethyl-6-methyl-5-(2-methylthiazol-4-yl)pyridazin-3(2H)-one 6

A suspension of **5** (0.65 mmol) and thioacetamide (0.65 mmol) in 5 mL of ethanol was refluxed for 1 h. After cooling, ice-cold water was added and the suspension was extracted with CH₂Cl₂ (3 × 10 mL). After evaporation of the solvent, the final compound was recovered and purified by crystallization from ethanol. Yield = 77%; mp = 134–136°C (EtOH). ¹H-NMR (400 MHz, CDCl₃) δ 7.25 (s, 1H, Ar), 5.85 (exch br s, 2H, NH₂), 4.20 (q, J = 7.2 Hz, 2H, CH₂), 2.78 (s, 3H, CH₃), 2.61 (s, 3H, C6-CH₃), 1.37 (t, J = 7.2 Hz, 3H, CH₃). Anal. Calcd C₁₁H₁₄N₄OS (250.32): C, 52.78; H, 5.63; N, 22.38; found: C, 52.92; H, 5.63; N, 22.44.

4.1.7 | General procedure for the synthesis of compounds **7a,b**

A mixture of compound **6** (0.44 mmol), suitable arylboronic acid (0.88 mmol), anhydrous cupric acetate (0.66 mmol), triethylamine (0.88 mmol), and activated molecular sieves (700 mg, 4 Å) in dry dichloromethane (10 mL) was stirred at room temperature for 5–24 h. The reaction mixture was filtered and washed with 33% NH₃ (5 mL × 2) and with water (10 mL × 2). The solvent was removed under reduced pressure. The resulting residue was purified by crystallization from ethanol.

4-[[2-Ethyl-6-methyl-5-(2-methylthiazol-4-yl)-3-oxo-2,3-dihydropyridazin-4-yl]amino]benzonitrile (7a)

Yellow-colored solid, mp = 196–198°C (EtOH). Yield = 50%. ¹H-NMR (400 MHz, CDCl₃) δ 7.82 (exch br s, 1H, NH), 7.29 (s, 2H, Ar), 6.82

(s, 1H, Ar), 6.73 (d, $J = 8.7$ Hz, 2H, Ar), 4.27 (q, $J = 7.2$ Hz, 2H, CH₂), 2.60 (s, 3H, CH₃), 2.26 (s, 3H, CH₃), 1.43 (t, $J = 7.2$ Hz, 3H, CH₃). ¹³C-NMR (100 MHz, CDCl₃) δ 188.83, 177.62, 167.83, 152.74, 143.14, 132.17, 120.79, 120.59, 119.02, 114.99, 47.61, 21.31, 18.98, 13.65. MS-ESI for C₁₈H₁₇N₅OS (calcd. 351.12), [M+H]⁺ at m/z 351.98, $t_R = 12.345$. Anal. Calcd C₁₈H₁₇N₅OS (351.43): C, 61.52; H, 4.88; N, 19.93; found: C, 61.68; H, 4.89; N, 19.98.

2-Ethyl-6-methyl-5-(2-methylthiazol-4-yl)-4-[(3,4,5-trifluorophenyl)amino]pyridazin-3(2H)-one (**7b**)

Yield = 32%; mp = 162–164°C (EtOH). ¹H-NMR (400 MHz, CDCl₃) δ 7.62 (exh br s, 1H, NH), 6.73 (s, 1H, Ar), 6.35 (m, 2H, Ar), 4.23 (q, $J = 7.4$ Hz, 2H, CH₂), 2.61 (s, 3H, CH₃), 2.17 (s, 3H, C6-CH₃), 1.41 (t, $J = 7.4$ Hz, 3H, CH₃). Anal. Calcd C₁₇H₁₅F₃N₄OS (380.39): C, 53.68; H, 3.97; N, 14.73; found: C, 53.54; H, 3.98; N, 14.70.

4.1.8 | Synthesis of 7-ethoxy-3-methyl-4-phenylisoxazolo[3,4-d]pyridazine **9b**

A solution of compound **8**^[26] (0.38 mmol) and EtONa (5 mmol) in 10 mL of absolute EtOH was stirred at room temperature for 3 h. After neutralization with acetic acid, the mixture was concentrated to a reduced volume. After cooling, the precipitate was recovered by suction and recrystallized from ethanol. Yield = 85%; mp > 300°C (EtOH). ¹H-NMR (400 MHz, CDCl₃) δ 7.65–7.54 (m, 5H, Ar), 4.80 (q, $J = 7.2$ Hz, 2H, CH₂), 2.69 (s, 3H, CH₃), 1.58 (t, $J = 7.0$ Hz, 3H, CH₃). Anal. Calcd C₁₄H₁₃N₃O₂ (255.10): C, 65.87; H, 5.13; N, 16.46; found: C, 66.05; H, 5.14; N, 16.49.

4.1.9 | General procedure for the synthesis of compounds **10a,b**

Compounds **9a,b** (0.60 mmol) were subjected to catalytic reduction with 10% Pd/C (0.06 mmol) in EtOH (30 mL) for 5 h in a Parr instrument at 60 PSI. The catalyst was filtered off and the solvent was evaporated under vacuum to obtain the desired final compounds which were crystallized from ethanol.

1-(5-Amino-6-methoxy-3-phenylpyridazin-4-yl)ethan-1-one (**10a**)

Yield = 76%; mp = 88–91°C (EtOH). ¹H-NMR (400 MHz, CDCl₃) δ 7.58–7.54 (m, 5H, Ar), 1.84 (s, 3H, COCH₃), 6.44 (exch br s, 2H, NH₂), 4.20 (s, 3H, OCH₃). Anal. Calcd C₁₃H₁₃N₃O₂ (243.27): C, 64.19; H, 5.39; N, 17.27; found: C, 64.01; H, 5.41; N, 17.31.

1-(5-Amino-6-ethoxy-3-phenylpyridazin-4-yl)ethan-1-one (**10b**)

Yield = 82%; mp = 94–96°C (EtOH). ¹H-NMR (400 MHz, CDCl₃) δ 7.54–7.47 (m, 5H, Ar), 6.42 (exch br s, 2H, NH₂), 4.66 (q, $J = 7.0$ Hz, 2H, CH₂), 1.78 (s, 3H, COCH₃), 1.51 (s, $J = 7.0$ Hz, 3H, CH₃). Anal. Calcd C₁₄H₁₅N₃O₂ (257.29): C, 65.36; H, 5.88; N, 16.33; found: C, 65.54; H, 5.87; N, 16.37.

4.1.10 | General procedure for the synthesis of compounds **11a,b**

Compounds **11a,b** were obtained from **10a,b** through the same procedures described for **7a,b**. For these compounds, the mixture was stirred at room temperature for 1–2 h and the final compounds were purified by crystallization from cyclohexane.

1-[5-[(3-Chlorophenyl)amino]-6-methoxy-3-phenylpyridazin-4-yl]ethan-1-one (**11a**)

Yellow-colored solid, mp = 124–126°C (CHX). Yield = 70%. ¹H-NMR (400 MHz, CDCl₃) δ 7.79 (s, 1H, NH), 7.58–7.49 (m, 5H, Ar), 7.29 (d, $J = 8.8$ Hz, 1H, Ar), 7.20 (d, $J = 8.1$ Hz, 1H, Ar), 7.03 (s, 1H, Ar), 6.94 (d, $J = 8.1$ Hz, 1H, Ar), 4.11 (s, 3H, CH₃), 1.82 (s, 3H, CH₃). ¹³C-NMR (100 MHz, CDCl₃) δ 156.09, 154.37, 140.04, 134.75, 134.16, 132.21, 130.88, 130.65, 130.14, 129.36, 129.31, 129.22, 129.02, 128.88, 126.37, 123.59, 121.68, 56.03, 31.74. MS-ESI for C₁₉H₁₆ClN₃O₂ (calcd. 353.09), [M+H]⁺ at m/z 353.94, $t_R = 11.609$. Anal. Calcd C₁₉H₁₆ClN₃O₂ (253.81): C, 64.50; H, 4.56; N, 11.88; found: C, 64.68; H, 4.57; N, 11.92.

1-[5-[(3-Chlorophenyl)amino]-6-ethoxy-3-phenylpyridazin-4-yl]ethan-1-one (**11b**)

Yield = 58%; mp = 118–120°C (CHX). ¹H-NMR (400 MHz, CDCl₃) δ 8.27 (exch br s, 1H, NH), 7.58–7.47 (m, 5H, Ar), 7.25–7.14 (m, 2H, Ar), 6.94 (m, 2H, Ar), 4.55 (q, $J = 7.0$ Hz, 2H, CH₂), 1.88 (s, 3H, COCH₃), 1.25 (t, $J = 7.0$ Hz, 3H, CH₃). Anal. Calcd C₂₀H₁₈ClN₃O₂ (367.83): C, 65.31; H, 4.93; N, 11.42; found: C, 65.47; H, 4.93; N, 11.47.

4.1.11 | General procedure for the synthesis of compounds **13h-j**

The suitable 2- or 4-substituted benzaldehyde (0.90 mmol) was added to a solution of **12a,b**^[27] (0.90 mmol) in 3.5 mL of KOH 5% (w/v) in absolute EtOH and the mixture was refluxed under stirring for 1–2 h. After cooling, the sample was concentrated in vacuo, diluted with ice-cold water (10–15 mL) and acidified with 2 N HCl. The precipitate was recovered by suction and finally purified by crystallization from ethanol.

4-(3-Chlorobenzyl)-6-(4-fluorophenyl)pyridazin-3(2H)-one (**13h**)

Yield = 88%; mp = 184–185°C (EtOH). ¹H-NMR (400 MHz, CDCl₃) δ 11.25 (exch br s, 1H, NH), 7.72–7.65 (m, 2H, Ar), 7.31–7.08 (m, 7H, Ar), 3.98 (s, 2H, CH₂). Anal. Calcd C₁₇H₁₂ClFN₂O (314.06): C, 64.87; H, 3.84; N, 8.90; found: C, 64.99; H, 3.84; N, 8.92.

2-[(3-Oxo-6-phenyl-2,3-dihydropyridazin-4-yl)methyl]benzoic acid (**13i**)

Yield = 56%; mp = 188–191°C (EtOH). ¹H-NMR (400 MHz, CDCl₃) δ 8.01 (m, 1H, Ar), 7.78–7.50 (m, 4H, Ar), 7.45 (m, 5H, Ar), 4.10 (s, 2H,

CH₂). Anal. Calcd C₁₈H₁₄N₂O₃ (306.32): C, 70.58; H, 4.61; N, 9.15 found: C, 70.47; H, 4.62; N, 9.17.

4-[(3-Oxo-6-phenyl-2,3-dihydropyridazin-4-yl)methyl]benzoic acid (**13j**)

Yield = 60%; mp = 198–200°C (EtOH). ¹H-NMR (400 MHz, CDCl₃) δ 8.01 (s, 1H, Ar), 7.80–7.48 (m, 4H, Ar), 7.41 (m, 5H, Ar), 3.98 (s, 2H, CH₂). Anal. Calcd C₁₈H₁₄N₂O₃ (306.32): C, 70.58; H, 4.61; N, 9.15 found: C, 70.49; H, 4.61; N, 9.13.

4.1.12 | General procedure for the synthesis of compounds **14a–h**

A suspension of the suitable **13a–h**^[28–32] (0.86 mmol), K₂CO₃ (1.72 mmol), and ethyl bromide (1.72 mmol) in anhydrous DMF (2–3 mL) was stirred at 80°C for 1 h. After cooling, the mixture was diluted with cold water and the precipitate was recovered by suction. For compounds **14a**, **14d**, and **14g**, the suspension was extracted with CH₂Cl₂ (3 × 10 mL) and, after evaporation of the solvent, the final compounds were crystallized from ethanol.

4-Benzyl-2-ethyl-6-phenylpyridazin-3(2H)-one (**14a**)

Yellow-colored solid, mp = 102–104°C (EtOH). Yield = 40%. ¹H-NMR (400 MHz, CDCl₃) δ 7.54 (d, *J* = 7.8 Hz, 2H, Ar), 7.28–7.21 (m, 5H, Ar), 7.17–7.13 (m, 3H, Ar), 7.10 (s, 1H, Ar), 4.20 (q, *J* = 7.2 Hz, 2H, CH₂), 3.85 (s, 2H, CH₂), 1.33 (t, *J* = 7.2 Hz, 3H, CH₃). ¹³C-NMR (100 MHz, CDCl₃) δ 160.22, 144.35, 143.41, 137.53, 135.53, 129.66, 129.25, 128.96, 127.02, 126.89, 126.07, 47.59, 36.45, 13.81. MS-ESI for C₁₉H₁₈N₂O (calcd. 290.14), [M+H]⁺ at *m/z* 291.01, *t_R* = 17.402. Anal. Calcd C₁₉H₁₈N₂O (290.37): C, 78.59; H, 6.25; N, 9.65; found: C, 78.37; H, 6.24; N, 9.67.

2-Ethyl-4-(3-fluorobenzyl)-6-phenylpyridazin-3(2H)-one (**14b**)

Yellow-colored solid, mp = 92–94°C (EtOH). Yield = 77%. ¹H-NMR (400 MHz, CDCl₃) δ 7.70–7.67 (m, 2H, Ar), 7.48–7.37 (m, 4H, Ar), 7.32 (q, *J* = 6.0 Hz, 1H, Ar), 7.08 (d, *J* = 7.6 Hz, 1H, Ar), 7.02–6.95 (m, 2H, Ar), 4.33 (q, *J* = 7.2 Hz, 2H, CH₂), 3.97 (s, 2H, CH₂), 1.46 (t, *J* = 7.2 Hz, 3H, CH₃). ¹³C-NMR (100 MHz, CDCl₃) δ 144.34, 142.56, 140.09, 140.02, 135.39, 130.45, 130.37, 129.35, 129.00, 127.04, 126.07, 125.29, 125.26, 116.58, 116.37, 114.12, 113.91, 47.65, 36.23, 13.80. MS-ESI for C₁₉H₁₇FN₂O (calcd. 308.13), [M+H]⁺ at *m/z* 309.00, *t_R* = 17.623. Anal. Calcd C₁₉H₁₇FN₂O (308.36): C, 74.01; H, 5.56; N, 9.08; found: C, 74.22; H, 5.57; N, 9.06.

4-(3-Chlorobenzyl)-2-ethyl-6-phenylpyridazin-3(2H)-one (**14c**)

Yellow-colored solid, mp = 117–119°C (EtOH). Yield = 46%. ¹H-NMR (400 MHz, CDCl₃) δ 7.70–7.66 (m, 2H, Ar), 7.44–7.36 (m, 3H, Ar), 7.28–7.25 (m, 4H, Ar), 7.20–7.18 (m, 1H, Ar), 4.32 (q, *J* = 7.2 Hz, 2H, CH₂), 3.94 (s, 2H, CH₂), 1.44 (t, *J* = 7.2 Hz, 3H, CH₃). ¹³C-NMR (100 MHz, CDCl₃) δ 160.03, 144.34, 142.45, 139.62, 135.37, 134.69, 130.18, 129.59, 129.36, 129.01, 127.82, 127.29, 127.10, 126.08, 47.65, 36.18, 13.80. MS-ESI for C₁₉H₁₇ClN₂O (calcd. 324.10),

[M+H]⁺ at *m/z* 324.96, *t_R* = 18.607. Anal. Calcd C₁₉H₁₇ClN₂O (324.81): C, 70.26; H, 5.28; N, 8.62; found: C, 70.50; H, 5.27; N, 8.60.

4-(3-Bromobenzyl)-2-ethyl-6-phenylpyridazin-3(2H)-one (**14d**)

Yellow-colored solid, mp = 118–120°C (EtOH). Yield = 47%. ¹H-NMR (400 MHz, CDCl₃) δ 7.69 (d, *J* = 5.6 Hz, 2H, Ar), 7.42 (d, *J* = 11.1 Hz, 6H, Ar), 7.25–7.20 (m, 3H, Ar), 4.31 (q, *J* = 7.2 Hz, 2H, CH₂), 3.93 (s, 2H, CH₂), 1.44 (t, *J* = 7.2 Hz, 3H, CH₃). ¹³C-NMR (100 MHz, CDCl₃) δ 160.02, 144.35, 142.43, 139.93, 135.37, 132.48, 130.47, 130.21, 129.37, 129.02, 128.29, 127.12, 126.09, 122.93, 47.66, 36.15, 13.80. MS-ESI for C₁₉H₁₇BrN₂O (calcd. 368.05), [M+H]⁺ at *m/z* 368.86, *t_R* = 10.813. Anal. Calcd C₁₉H₁₇BrN₂O (369.26): C, 61.80; H, 4.64; N, 7.59; found: C, 61.97; H, 4.66; N, 7.62.

2-Ethyl-4-(3-methoxybenzyl)-6-phenylpyridazin-3(2H)-one (**14e**)

Yellow-colored solid, mp = 88–90°C (EtOH). Yield = 55%. ¹H-NMR (400 MHz, CDCl₃) δ 7.68–7.66 (m, 2H, Ar), 7.43–7.36 (m, 3H, Ar), 7.29–7.28 (m, 1H, Ar), 7.25 (s, 1H, Ar), 6.88–6.87 (m, 1H, Ar), 6.83–6.82 (m, 2H, Ar), 4.33 (q, *J* = 7.2 Hz, 2H, CH₂), 3.95 (s, 2H, CH₂), 3.80 (s, 3H, OCH₃), 1.46 (t, *J* = 7.2 Hz, 3H, CH₃). ¹³C-NMR (100 MHz, CDCl₃) δ 160.21, 160.08, 144.39, 143.24, 139.11, 135.53, 129.95, 129.26, 128.96, 126.94, 126.10, 122.00, 115.35, 112.38, 55.37, 47.62, 36.44, 13.82. MS-ESI for C₂₀H₂₀N₂O₂ (calcd. 320.15), [M+H]⁺ at *m/z* 320.97, *t_R* = 17.354. Anal. Calcd C₂₀H₂₀N₂O₂ (320.39): C, 74.98; H, 6.29; N, 8.74; found: C, 74.72; H, 6.28; N, 8.71.

2-Ethyl-4-(2-methoxybenzyl)-6-phenylpyridazin-3(2H)-one (**14f**)

Yellow-colored solid, mp = 89–91°C (EtOH). Yield = 95%. ¹H-NMR (400 MHz, CDCl₃) δ 7.67–7.63 (m, 2H, Ar), 7.42–7.36 (m, 3H, Ar), 7.28 (s, 1H, Ar), 7.27–7.26 (m, 1H, Ar), 7.19–7.18 (m, 1H, Ar), 6.98–6.91 (m, 2H, Ar), 4.33 (q, *J* = 7.2 Hz, 2H, CH₂), 3.98 (s, 2H, CH₂), 3.80 (s, 3H, OCH₃), 1.46 (t, *J* = 7.2 Hz, 3H, CH₃). ¹³C-NMR (100 MHz, CDCl₃) δ 160.42, 157.82, 144.36, 142.77, 135.78, 131.61, 129.11, 128.91, 128.53, 126.45, 126.05, 125.72, 120.95, 110.77, 55.50, 47.51, 31.01, 13.83. MS-ESI for C₂₀H₂₀N₂O₂ (calcd. 320.15), [M+H]⁺ at *m/z* 320.97, *t_R* = 17.781. Anal. Calcd C₂₀H₂₀N₂O₂ (320.39): C, 74.98; H, 6.29; N, 8.74; found: C, 74.76; H, 6.27; N, 8.76.

2-Ethyl-4-(naphthalen-2-ylmethyl)-6-phenylpyridazin-3(2H)-one (**14g**)

Yield = 56%; oil. ¹H-NMR (400 MHz, CDCl₃) δ 7.87 (m, 3H, Ar), 7.49 (m, 6H, Ar), 7.31 (m, 3H, Ar), 6.96 (s, 1 H, Ar), 4.47–4.40 (m, 4H, 2 × CH₂), 1.53 (t, *J* = 7.2 Hz, 3H, CH₃). Anal. Calcd C₂₀H₂₀N₂O (340.43): C, 81.15; H, 5.92; N, 8.23; found: C, 81.40; H, 5.91; N, 8.24.

4-(3-Chlorobenzyl)-2-ethyl-6-(4-fluorophenyl)pyridazin-3(2H)-one (**14h**)

Yellow-colored solid, mp = 127–129°C (EtOH). Yield = 74%. ¹H-NMR (400 MHz, CDCl₃) δ 7.69–7.66 (m, 2H, Ar), 7.27 (s, 2H, Ar), 7.22–7.09 (m, 5H, Ar), 4.31 (q, *J* = 7.2 Hz, 2H, CH₂), 3.94 (s, 2H, CH₂), 1.44 (t, *J* = 7.2 Hz, 3H, CH₃). ¹³C-NMR (100 MHz, CDCl₃) δ 164.85,

162.37, 159.88, 143.40, 142.66, 139.53, 134.72, 130.20, 129.58, 128.01, 127.92, 127.82, 127.34, 126.78, 116.12, 115.91, 47.65, 36.18, 13.79. MS-ESI for $C_{19}H_{16}ClFN_2O$ (calcd. 342.09), $[M+H]^+$ at m/z 342.95, $t_R = 18.676$. Anal. Calcd $C_{19}H_{16}ClFN_2O$ (342.80): C, 66.57; H, 4.70; N, 8.17; found: C, 66.76; H, 4.70; N, 8.19.

4.1.13 | Synthesis of 4-(3-chlorobenzyl)-2-ethyl-6-phenylpyridazine-3(2H)-thione 15

To a suspension of **14c** (0.37 mmol) in anhydrous toluene (5 mL) 1.11 mmol of Lawesson's reagent were added and the mixture was refluxed for 7 h. After cooling, the solvent was evaporated in vacuo. The residue was diluted with cold water (15 mL) and extracted with CH_2Cl_2 (3×15 mL). After evaporation of the solvent, the final product was purified by flash chromatography using toluene/ethyl acetate 8:2 as eluent. Yield = 28%; mp = 81–83°C (EtOH). 1H -NMR (400 MHz, $CDCl_3$) δ 7.78 (m, 2H, Ar), 7.52 (m, 3H, Ar), 7.36 (m, 3H, Ar), 7.28–7.14 (m, 1H, Ar), 7.06 (s, 1H, Ar), 4.95 (q, $J = 7.2$ Hz, 2H, CH_2), 4.26 (s, 2H, CH_2), 1.63 (t, $J = 7.2$ Hz, 3H, CH_3). Anal. Calcd $C_{19}H_{17}ClN_2S$ (340.87): C, 66.95; H, 5.03; N, 8.22; found: C, 67.11; H, 5.04; N, 8.25.

4.1.14 | General procedure for the synthesis of compounds 16a,b

Compounds **16a,b** were obtained from **13i** and **13j** respectively, through the same procedure described for **14a–h**. The suspension was extracted with CH_2Cl_2 (3×10 mL) and, after evaporation of the solvent, the final compounds were recrystallized from ethanol.

Ethyl 4-[(2-ethyl-3-oxo-6-phenyl)-2,3-dihydropyridazin-4-yl)methyl] benzoate (16a)

Yield = 64%; mp = 64–66°C (EtOH). 1H -NMR (400 MHz, $CDCl_3$) δ 8.04 (d, $J = 8.4$ Hz, 2H, Ar), 7.66 (m, 2H, Ar), 7.43–7.35 (m, 5H, Ar), 7.24 (s, 1H, Ar), 4.41–4.28 (m, 4H, $2 \times CH_2$), 4.04 (s, 2H, CH_2), 1.49–1.36 (m, 6H, $2 \times CH_3$). Anal. Calcd $C_{22}H_{22}N_2O_3$ (362.43): C, 72.91; H, 6.12; N, 7.73; found: C, 72.71; H, 6.14; N, 7.75.

Ethyl 2-[(2-ethyl-3-oxo-6-phenyl)-2,3-dihydropyridazin-4-yl)methyl] benzoate (16b)

Yellow-colored solid, mp = 77–79°C (EtOH). Yield = 98%. 1H -NMR (400 MHz, $CDCl_3$) δ 8.01–7.98 (m, 1H, Ar), 7.63–7.61 (m, 2H, Ar), 7.53–7.49 (m, 1H, Ar), 7.39–7.33 (m, 5H, Ar), 7.11 (s, 1H, Ar), 4.36–4.24 (m, 6H, CH_2), 1.46 (t, $J = 7.2$ Hz, 3H, CH_3), 1.27 (t, $J = 7.2$ Hz, 3H, CH_3). ^{13}C -NMR (100 MHz, $CDCl_3$) δ 167.39, 160.13, 144.34, 143.48, 138.74, 135.65, 132.51, 131.20, 130.84, 129.15, 128.90, 127.31, 126.51, 126.07, 61.22, 47.56, 34.92, 14.25, 13.83. MS-ESI for $C_{22}H_{22}N_2O_3$ (calcd. 362.16), $[M+H]^+$ at m/z 362.97, $t_R = 10.065$. Anal. Calcd $C_{22}H_{22}N_2O_3$ (362.43): C, 72.91; H, 6.12; N, 7.73; found: C, 72.75; H, 6.13; N, 7.71.

4.1.15 | Synthesis of 4-[(2-ethyl-3-oxo-6-phenyl)-2,3-dihydropyridazin-4-yl)methyl]benzoic acid 17

A solution of **16a** (0.27 mmol) in 6 mL of EtOH and 4 mL of 6 N NaOH was stirred at room temperature for 1 h. After evaporation of the solvent, cold water was added and the solution was acidified with 6 N HCl. The precipitate was recovered by suction and recrystallized from ethanol. Yellow-colored solid, mp = 110–112°C (EtOH). Yield = 88%. 1H -NMR (400 MHz, $CDCl_3$) δ 8.09 (d, $J = 8.2$ Hz, 2H, Ar), 7.69 (d, $J = 8.1$ Hz, 2H, Ar), 7.41 (d, $J = 7.6$ Hz, 5H, Ar), 7.28 (s, 1H, Ar), 4.34 (q, $J = 7.2$ Hz, 2H, CH_2), 4.06 (s, 2H, CH_2), 1.46 (t, $J = 7.2$ Hz, 3H, CH_3). ^{13}C -NMR (100 MHz, $CDCl_3$) δ 171.03, 160.12, 144.50, 143.84, 142.29, 135.25, 130.86, 129.74, 129.42, 129.03, 128.24, 127.29, 126.07, 47.78, 36.64, 13.80. MS-ESI for $C_{20}H_{18}N_2O_3$ (calcd. 334.13), $[M+H]^+$ at m/z 334.97, $t_R = 14.665$. Anal. Calcd $C_{20}H_{18}N_2O_3$ (334.38): C, 71.84; H, 5.43; N, 8.38; found: C, 71.65; H, 5.42; N, 8.40.

4.2 | Pharmacological assays: FABP inhibitory activity assays

A displacement test was used to evaluate the FABP4 ligands' inhibitory efficacy in accordance with the Cayman's instructions for their FABP4 Inhibitor/Ligand Screening Assay Kit, item 10010231. The samples of compounds to be tested for activity against FABP4 were prepared as stock solutions (1 mM) in DMSO. On the day of assay, the compounds were all diluted in phosphate buffer solution (PBS, pH 7.4) to the following concentrations: 100, 50, 10, 5, 2, 1, and 0 μ M. Appropriate concentrations of DMSO in PBS were used as a control. The Cayman's DR (FABP Assay Detection Reagent, Item 10010376) included in the kit was utilized in the experiments. FABP4 protein from the kit was combined with the DR, which was diluted before being incubated for 10 min at room temperature. Then, after another 10 min of equilibration, compounds were introduced to record the activity. The fluorescence signal was recorded at 470 nm (i.e., emission, with the excitation fixed at 370 nm) with a CytoFluor[®] Series 4000 Fluorescence Multi-Well Plate Reader. The IC_{50} was determined in accordance with the instructions in the kit manual for Cayman Chemicals' FABP4 Inhibitor/Ligand Screening Assay Kit (Item No. 10010231), which are as follows: (1) determine each sample's average fluorescence; (2) by deducting the blank, determine the background corrected fluorescence (BCF); (3) divide the BCF of each sample by the maximum BCF and multiply by 100% (this is the value in percent fluorescence units, i.e. % FU); (4) plot the % FU values against the concentration of inhibitor/ligand used; (5) find the concentration of inhibitor/ligand that corresponds to 50% FU, to determine IC_{50} values.

4.3 | Molecular docking

Marvin Sketch was used to create the 2D chemical structures, and the same software's MMFF94 force field was used to apply molecular mechanics energy minimization to each structure.^[35] The three-dimensional (3D) geometry of all compounds was then optimized using

the PM3 Hamiltonian,^[36] as implemented in MOPAC 2016 package assuming a pH of 7.0.^[37] Once built and optimized, all structures were used in the bioisostere replacement tool Spark 10.4.0.^[36,38] The replacement/growing was performed using the same 178,558 fragments for each part; in particular, the fragments derive from ChEMBL and Zinc databases with a protocol already reported and validated.^[16,39–42] Using AutoDock's default docking parameters and a validated protocol, docking calculations were performed.^[40] The setup was done with YASARA. The Lamarckian genetic algorithm implemented in AutoDock was used for the calculations. The ligand-centered maps were generated by AutoGrid with a spacing of 0.375 Å and dimensions that encompass all atoms extending 5 Å from the surface of the ligand. All of the parameters were inserted at their default settings. PDBid: 1TOU and 3WBG were downloaded from the Protein Data Bank (www.rcsb.org), and used for the calculations. MM/PBSA rescoring procedures were obtained by using fastDRH as open access web server (<http://cadd.zju.edu.cn/fastdrh/overview>, accessed on December 05, 2022).^[43] The molecular dynamics simulations of the complexes were performed with the YASARA. A periodic simulation cell extending 10 Å from the surface of the protein was employed. The cell was filled with water, with a maximum sum of all water bumps of 1.0 Å and a density of 0.997 g/mL. The setup included optimizing the hydrogen bonding network^[44] to increase the solute stability and a pK_a prediction to fine-tune the protonation states of protein residues at the chosen pH of 7.4.^[45] With an excess of either Na or Cl to neutralize the cell, NaCl ions were supplied at a physiological concentration of 0.9%. The simulation was run using the ff14SB force field^[46] for the solute, GAFF2,^[47] AM1BCC^[48] for ligands, and TIP3P for water. The cutoff was 10 Å for Van der Waals forces (the default used by AMBER),^[49] and no cutoff was applied to electrostatic forces (using the Particle Mesh Ewald algorithm).^[50] The equations of motions were integrated with multiple time steps of 2.5 fs for bonded interactions and 5.0 fs for nonbonded interactions at a temperature of 298 K and a pressure of 1 atm using algorithms described in detail previously.^[51] Short MD simulation was run on the solvent only to remove clashes. The entire system was then energy minimized using a steepest descent minimization to remove conformational stress, followed by a simulated annealing minimization until convergence (<0.01 kcal/mol Å). Finally, 100 ns MD simulation without any restrictions was conducted, and the conformations were recorded every 200 ps.

ACKNOWLEDGMENTS

This research has received funding for a scholarship to R.R.d.O.S from the Coordination for the Improvement of Higher Education Personnel—Brazil (CAPES-PRINT, funding number 88887.570120/2020-00).

CONFLICTS OF INTEREST STATEMENT

The authors declare no conflicts of interest.

ORCID

Giuseppe Floresta  <http://orcid.org/0000-0002-0668-1260>

Letizia Crocetti  <http://orcid.org/0000-0003-3473-2683>

Vincenzo Patamia  <http://orcid.org/0000-0002-0048-2631>

Claudia Vergelli  <http://orcid.org/0000-0001-9774-8047>

Agostino Cilibrizzi  <http://orcid.org/0000-0002-9711-5183>

REFERENCES

- [1] U. Das, *Curr. Pharm. Biotechnol.* **2006**, 7(6), 467.
- [2] M. Furuhashi, G. S. Hotamisligil, *Nat. Rev. Drug Discov.* **2008**, 7, 489.
- [3] G. Boden, *Front. Biosci.* **1998**, 3, d169.
- [4] G. S. Hotamisligil, D. A. Bernlohr, *Nat. Rev. Endocrinol.* **2015**, 11(10), 592.
- [5] J. Storch, A. E. A. Thumser, *Biochim. Biophys. Acta Mol. Cell Biol. Lipids* **2000**, 1486(1), 28.
- [6] G. Floresta, V. Pistarà, E. Amata, M. Dichiarà, A. Marrazzo, O. Prezzavento, A. Rescifina, *Eur. J. Med. Chem.* **2017**, 138, 854.
- [7] K. M. Nieman, H. A. Kenny, C. V. Penicka, A. Ladanyi, R. Buell-Gutbrod, M. R. Zillhardt, I. L. Romero, M. S. Carey, G. B. Mills, G. S. Hotamisligil, S. D. Yamada, M. E. Peter, K. Gwin, E. Lengyel, *Nat. Med.* **2011**, 17(11), 1498.
- [8] A. Tolle, S. Suhail, M. Jung, K. Jung, C. Stephan, *BMC Cancer* **2011**, 11, 302.
- [9] H. Uehara, T. Takahashi, M. Oha, H. Ogawa, K. Izumi, *Int. J. Cancer* **2014**, 135(11), 2558.
- [10] A. Yang, H. Zhang, Y. Sun, Y. Wang, X. Yang, X. Yang, H. Zhang, W. Guo, G. Zhu, J. Tian, Y. Jia, Y. Jiang, *Placenta* **2016**, 46, 49.
- [11] W. Tian, W. Zhang, Y. Zhang, T. Zhu, Y. Hua, H. Li, Q. Zhang, M. Xia, *Cancer Cell Int.* **2020**, 20, 512.
- [12] K. M. Gharpure, S. Pradeep, M. Sans, R. Rupaimoole, C. Ivan, S. Y. Wu, E. Bayraktar, A. S. Nagaraja, L. S. Mangala, X. N. Zhang, M. Haemmerle, W. Hu, C. Rodriguez-Aguayo, M. McGuire, C. S. L. Mak, X. H. Chen, M. A. Tran, A. Villar-Prados, G. A. Pena, R. Kondetimmanahalli, R. Nini, P. Koppula, P. Ram, J. S. Liu, G. Lopez-Berestein, K. Baggerly, L. S. Eberlin, A. K. Sood, *Nat. Commun.* **2018**, 9, 2923.
- [13] G. Floresta, V. Patamia, C. Zagni, A. Rescifina, *Eur. J. Med. Chem.* **2022**, 240, 114604.
- [14] G. Floresta, A. Cilibrizzi, V. Abbate, A. Spampinato, C. Zagni, A. Rescifina, *Data Brief* **2019**, 22, 471.
- [15] G. Floresta, D. Gentile, G. Perrini, V. Patamia, A. Rescifina, *Mar. Drugs* **2019**, 17(11), 624.
- [16] G. Floresta, A. Cilibrizzi, V. Abbate, A. Spampinato, C. Zagni, A. Rescifina, *Bioorg. Chem.* **2019**, 84, 276.
- [17] L. Crocetti, G. Floresta, S. Nazir, C. Vergelli, A. Bhogal, C. Biancalani, N. Cesari, M. P. Giovannoni, A. Cilibrizzi, *Struct. Chem.* **2022**, 33(3), 769.
- [18] G. Floresta, L. Crocetti, M. P. Giovannoni, P. Biagini, A. Cilibrizzi, *J. Enzyme Inhib. Med. Chem.* **2020**, 35(1), 1137.
- [19] L. Crocetti, G. Floresta, C. Zagni, D. Merugu, F. Mazzacuva, R. R. de Oliveira Silva, C. Vergelli, M. P. Giovannoni, A. Cilibrizzi, *Pharmaceuticals* **2022**, 15(11), 1335.
- [20] M. P. Giovannoni, C. Vergelli, A. Cilibrizzi, L. Crocetti, C. Biancalani, A. Graziano, V. D. Piaz, M. I. Loza, M. I. Cadavid, J. L. Díaz, *Bioorg. Med. Chem.* **2010**, 18(22), 7890.
- [21] M. P. Giovannoni, G. Ciciani, A. Cilibrizzi, L. Crocetti, S. Daniele, L. Di Cesare Mannelli, C. Ghelardini, C. Giacomelli, G. Guerrini, C. Martini, M. L. Trincavelli, C. Vergelli, *Eur. J. Med. Chem.* **2015**, 89, 32.
- [22] P. Biagini, C. Biancalani, A. Graziano, N. Cesari, M. P. Giovannoni, A. Cilibrizzi, V. D. Piaz, C. Vergelli, L. Crocetti, M. Delcanale, E. Armani, A. Rizzi, P. Puccini, P. M. Gallo, D. Spinabelli, P. Caruso, *Bioorg. Med. Chem.* **2010**, 18(10), 3506.
- [23] V. Dal Piaz, G. Ciciani, G. Turco, *Synthesis* **1989**, 1989, 213.
- [24] V. Dal Piaz, M. C. Castellana, C. Vergelli, M. P. Giovannoni, A. Gavaldà, V. Segarra, J. Beleta, H. Ryder, J. M. Palacios, *J. Enzyme Inhib. Med. Chem.* **2002**, 17(4), 227.
- [25] C. Vergelli, I. A. Schepetkin, G. Ciciani, A. Cilibrizzi, L. Crocetti, M. P. Giovannoni, G. Guerrini, A. Iacovone, L. N. Kirpotina, A. I. Khlebnikov, R. D. Ye, M. T. Quinn, *Bioorg. Med. Chem.* **2016**, 24(11), 2530.

- [26] C. Vergelli, M. P. Giovannoni, S. Pieretti, A. D. Giannuario, V. D. Piaz, P. Biagini, C. Biancalani, A. Graziano, N. Cesari, *Bioorg. Med. Chem.* **2007**, *15*(16), 5563.
- [27] M. P. Giovannoni, I. A. Schepetkin, A. Cilibrizzi, L. Crocetti, A. I. Khlebnikov, C. Dahlgren, A. Graziano, V. Dal Piaz, L. N. Kirpotina, S. Zerbinati, C. Vergelli, M. T. Quinn, *Eur. J. Med. Chem.* **2013**, *64*, 512.
- [28] A. Husain, A. Ahmad, A. Bhandari, V. Ram, *J. Chil. Chem. Soc.* **2011**, *56*(3), 778.
- [29] Y.-L. Tsai, S. Syu, S.-M. Yang, U. Das, Y.-S. Fan, C.-J. Lee, W. Lin, *Tetrahedron* **2014**, *70*(34), 5038.
- [30] A. A. Shalaby, A. M. Youssef, W. A. Youssef, N. A. Shams, *J. Chin. Chem. Soc.* **1994**, *41*(4), 477.
- [31] M. S. Abdelbaset, M. H. Abdelrahman, S. N. A. Bukhari, A. M. Gouda, B. G. M. Youssif, M. Abdel-Aziz, G. Abuo-Rahma, *Bioorg. Chem.* **2021**, *107*, 104522.
- [32] C. G. Wermuth, G. Schlewer, J. J. Bourguignon, G. Maghioros, M. J. Bouchet, C. Moire, J. P. Kan, P. Worms, K. Biziere, *J. Med. Chem.* **1989**, *32*(3), 528.
- [33] M. Hirose, S. Sugiyama, H. Ishida, M. Niiyama, D. Matsuoka, T. Hara, E. Mizohata, S. Murakami, T. Inoue, S. Matsuoka, M. Murata, *J. Synchrotron Radiat.* **2013**, *20*(6), 923.
- [34] H. Su, Y. Zou, G. Chen, H. Dou, H. Xie, X. Yuan, X. Zhang, N. Zhang, M. Li, Y. Xu, *J. Med. Chem.* **2020**, *63*(8), 4090.
- [35] A. Cheng, S. A. Best, K. M. Merz, Jr., C. H. Reynolds, *J. Mol. Graph. Model.* **2000**, *18*(3), 273.
- [36] J. J. P. Stewart, *J. Mol. Model.* **2004**, *10*(2), 155.
- [37] J. J. P. Stewart, *J. Comput.-Aided Mol. Des.* **1990**, *4*(1), 1.
- [38] T. Cheeseright, M. Mackey, S. Rose, A. Vinter, *J. Chem. Inf. Model.* **2006**, *46*(2), 665.
- [39] G. Floresta, E. Amata, M. Dichiarà, A. Marrazzo, L. Salerno, G. Romeo, O. Prezzavento, V. Pittalà, A. Rescifina, *Chem. Med. Chem.* **2018**, *13*(13), 1336.
- [40] M. G. Varrica, C. Zagni, P. G. Mineo, G. Floresta, G. Monciino, V. Pistarà, A. Abbadessa, A. Nicosia, R. M. Castilho, E. Amata, A. Rescifina, *Eur. J. Med. Chem.* **2018**, *143*, 583.
- [41] G. Floresta, A. N. Fallica, L. Salerno, V. Sorrenti, V. Pittalà, A. Rescifina, *Bioorg. Chem.* **2021**, *117*, 105428.
- [42] G. Floresta, E. Amata, D. Gentile, G. Romeo, A. Marrazzo, V. Pittalà, L. Salerno, A. Rescifina, *Mar. Drugs* **2019**, *17*(2), 113.
- [43] Z. Wang, H. Pan, H. Sun, Y. Kang, H. Liu, D. Cao, T. Hou, *Brief. Bioinf* **2022**, *23*(5), 1373.
- [44] E. Krieger, R. L. Dunbrack, R. W. Hooft, B. Krieger, *Comput. Drug Discov. Design*, Springer, **2012**, pp. 405.
- [45] E. Krieger, J. E. Nielsen, C. A. E. M. Spronk, G. Vriend, *Journal of Molecular Graphics and Modelling* **2006**, *25*(4), 481.
- [46] J. Maier, C. Martinez, K. Kasavajhala, L. Wickstrom, K. Hauser, C. Simmerling, *J. Chem. Theory Comput [Internet]*, American Chemical Society (ACS), **2015**.
- [47] J. Wang, R. M. Wolf, J. W. Caldwell, P. A. Kollman, D. A. Case, *J. Comput. Chem.* **2004**, *25*(9), 1157.
- [48] A. Jakalian, D. B. Jack, C. I. Bayly, *J. Comp. Chem.* **2002**, *23*(16), 1623.
- [49] V. Hornak, R. Abel, A. Okur, B. Strockbine, A. Roitberg, C. Simmerling, *Proteins: Struct., Funct., Bioinf.* **2006**, *65*(3), 712.
- [50] U. Essmann, L. Perera, M. L. Berkowitz, T. Darden, H. Lee, L. G. Pedersen, *J. Chem. Phys.* **1995**, *103*(19), 8577.
- [51] E. Krieger, G. Vriend, *J. Comput. Chem.* **2015**, *36*(13), 996.

SUPPORTING INFORMATION

Additional supporting information can be found online in the Supporting Information section at the end of this article.

How to cite this article: G. Floresta, L. Crocetti, R. R. de O. Silva, V. Patamia, F. Mazzacuva, Y. C. S. Chen, C. Vergelli, A. Cilibrizzi, *Arch. Pharm.* **2023**;356:e2300314.
<https://doi.org/10.1002/ardp.202300314>